Beyond conformational control: effects of noncovalent interactions on electronic properties of conjugated polymers

Bin Liu,[1] Dario Rocca,[2] He Yan,[3] and Ding Pan[1, 3, 4, *]

[1]*Department of Physics, Hong Kong University of Science and Technology, Hong Kong, China*

[2]*Université de Lorraine & CNRS, Laboratoire de Physique et Chimie Théoriques (LPCT), F-54000 Nancy, France*

[3]*Department of Chemistry, The Hong Kong University of Science and Technology, Hong Kong, China*

[4]*HKUST Fok Ying Tung Research Institute, Guangzhou, China*

(Dated: June 28, 2021)

Abstract

Tuning the electronic properties of polymers is of great importance in designing highly efficient organic solar cells. Noncovalent intramolecular interactions have been often used as conformational control to enhance the planarity of polymers or molecules, which may reduce band gaps and promote charge transfer. However, it is little known if noncovalent interactions may alter the electronic properties of conjugated polymers through some mechanism other than the conformational control. Here, we studied the effects of various noncovalent interactions, including sulfur-nitrogen , sulfur-oxygen, sulfur-fluorine, oxygen-nitrogen, oxygen-fluorine, and nitrogen-fluorine, on the electronic properties of polymers with planar geometry using unconstrained and constrained density functional theory. We found that the sulfur-nitrogen intramolecular interaction may reduce the band gaps of polymers and enhance the charge transfer more obviously than other noncovalent interactions. Our findings are also consistent with the experimental data. For the first time, our study shows that noncovalent interactions may directly affect the electronic structure of polymers, which is not due to the enhancement of molecular planarity. Our work suggests a new mechanism to manipulate the electronic properties of polymers to design high-performance small-molecule-polymer and all-polymer solar cells.

INTRODUCTION

Organic solar cells (OSCs), which consist of heterojunctions of electron-donating and electron-accepting organic matters, have many promising properties; for example, they are inexpensive, environmentally friendly, lightweight, and flexible [1–5]. Recently, substantial progress in designing and synthesizing small-molecule-polymer solar cells, in which the electron donors are conjugated polymers, and the acceptors are non-fullerene small molecules, has boosted the power conversion efficiency up to about 18% [4, 6–11]. All-polymer solar cells, where conjugated polymers work as both electron donors and acceptors, also show a promising efficiency of nearly 16% [12, 13]. In molecular engineering of small-molecule-polymer or all-polymer solar cells, polymers must be carefully designed, so that electron donors and acceptors can match well [2]. Tens of thousands of donor-acceptor combinations are available, but the scientific community still largely relies on the trial-and-error approach [5]. Many fundamental electronic properties of polymers are not well understood.

Tuning the electronic properties of conjugated polymers plays an important role in optimizing the performance of OSCs. The widely used designing strategies include donor-acceptor copolymers [2, 3, 14], fluorination [15–18], and planar conformation locking [19–21] In particular, the high planarity of backbone chains of polymers facilitates electron delocalization and $\pi - \pi$ intermolecular interactions, which result in narrower HOMO-LUMO band gaps and fast charge transfer [3, 20]. A promising approach of improving the planarity and rigidity of organic molecules is to introduce some noncovalent interactions such as sulfur-nitrogen, sulfur-oxygen, and sulfur-fluorine interactions [19, 21–24]. Yu et al. introduced the sulfur-nitrogen interaction as a noncovalent conformational lock in a small molecular acceptor to significantly enhance the photovoltaic performance [23]. Xia et al. found that the sulfur-oxygen interaction has the similar effects in the donor-acceptor conjugated polymers [22]. Some theoretical studies also suggested that noncovalent interactions may enhance planarity of both conjugated polymers and small molecule acceptors[19, 25]. So far, most of

previous studies focus on how noncovalent interactions control the conformation of polymers, which may further alter electronic properties; however, it is not yet known if noncovalent interactions may directly affect the electronic properties of planar polymers.

In this study, we considered six common noncovalent interactions: sulfur-nitrogen (S-N), sulfur-oxygen (S-O), sulfur-fluorine (S-F), oxygen-nitrogen (O-N), oxygen-fluorine (O-F), and nitrogen-fluorine (N-F), in 48 polymer structures with planar geometry. We found that after introducing the noncovalent intramolecular interactions, the band gaps of most polymers decrease and the hole transfer rates increase; particularly the sulfur-nitrogen interaction has the largest effect. Our findings are also consistent with the experimental data. This study paves the way for understanding and manipulating the electronic properties of polymers, which will facilitate the design of high-performance organic solar cells.

RESULTS AND DISCUSSION

Fig. 1(a) shows the representative structures of conjugated polymers with the six noncovalent interactions. To compare the structures with and without the noncovalent interactions, we rotated the corresponding moieties around the inter-ring carbon-carbon bonds by 180° or swapped the side chains (see Fig. 1(a) and Fig. S1). Before and after the modification, we relaxed both atomic positions and the lengths of repeating units, and found that all the polymers have planar and rigid backbone geometries. The distances of the noncovalent pairs are smaller than the sum of the van der Waals radii of the corresponding atoms [26, 27], so the noncovalent interactions likely stabilize the polymer structures, which are consistent with previous studies [21].

We calculated the electronic structure of the polymers. Fig. 1(b) shows the change of HOMO-LUMO band gaps, ΔE_g , after introducing the noncovalent interactions. We found that the ΔE_g values are largely negative, among which the sulfur-nitrogen interaction reduces band gaps most. The sulfur atom is in the thiophene moiety, and the nitrogen atom

4

is from benzothiadiazole. We studied seven different polymer structures with the sulfur-nitrogen interaction (see Figs. S2 and S3 in the supporting information), whose ΔE_g can be as low as -0.15 eV. In our calculations, we used the vacuum energy level to align the HOMO and LUMO levels, and found that after introducing the sulfur-nitrogen interaction, the HOMO levels shift to higher energies, while the LUMO levels change little (see Fig S5 in the supporting information). Fig. 2(a) shows that the HOMO is distributed closer to the polymer backbone than the LUMO, which means that the sulfur-nitrogen interaction may affect the electronic state of the polymer backbone. We plotted the projected density of states of conjugated carbon atoms in Fig. 2 (c) and (d), showing that the HOMO is the π bonding orbital, made by the p_z orbitals of the conjugated carbon atoms. The change of the π bonding orbital along the backbone carbon atoms may affect transport properties of polymers.

We calculated the change of hole transfer rates of the polymers after introducing the noncovalent interactions in Fig. 3. Because polymers are often used as electron donors in the OSC devices, we mainly consider the hole transport in the hopping regime along the backbone chains. We applied the following adiabatic rate equation [20, 28]:

$$k^{Troisi} = \frac{\omega}{2\pi} \left[1 - \exp\left(\frac{-2\pi^{3/2}|H_{AB}|^2}{\hbar\omega\sqrt{\lambda k_B T}} \right) \right] \cdot \exp\left[-\frac{\lambda}{4k_B T} + \frac{|H_{AB}|}{k_B T} \right], \qquad (1)$$

where ω is the representative frequency for optical phonons (1000 cm^{-1}), H_{AB} is the non-adiabatic electronic couplings between the A and B states, λ is the reorganization energy, k_B is the Boltzmann constant and T is the temperature (298.15 K). We applied the constrained density functional theory (DFT) method to calculate H_{AB} along the backbone chains. Constrained DFT considers the effects of polarization and orbital relaxation, which are commonly found in the OSC applications [29, 30]. We manually localized charges in polymer moieties using the Becke constraint[31], and tested a few possible hopping pathways (see Figs. S6 and S7). The reorganization energy λ contains two parts:

$$\lambda = \lambda_{in} + \lambda_{ext}. \qquad (2)$$

λ_{in} is the internal reorganization energy, and can be calculated as [32]

$$\lambda = E_0(Q_+) - E_0(Q_0) + E_+(Q_0) - E_+(Q_+), \tag{3}$$

where Q_0 and Q_+ correspond to the optimized neutral and cationic polymer structures, respectively, $E_0(Q_+)$ is the energy of the neutral state calculated with the cationic structure, and $E_+(Q_0)$ is the energy of the cationic state calculated with the neutral structure. The external reorganization energy λ_{ext} accounts for the response of surrounding molecules in the charge-transfer process, which is 0.14 eV for all the polymers studied here [33]. While Marcus theory is widely used to calculate the charge hopping rates, because for the polymers studied here the non-adiabatic couplings (H_{AB}) are larger than $\lambda/2$, we applied Eq. (1) instead of Marcus theory [20, 28].

In Fig 3, we compared the hole transfer rates between the two nearest repeating moieties participating in the noncovalent interactions. The sulfur-nitrogen interaction increases the hole transfer rate by $10^2 \sim 10^7$ times, which is overall the largest among all the nonconvalent interactions studied here. The results suggest that the sulfur-nitrogen interaction does not only reduce band gaps, but also considerably improve transport properties.

To understand why the sulfur-nitrogen interaction changes band gaps and hole transfer rates most, we first examined the intramolecular charge transfer using the Mulliken population analysis. We found that after the thiophene sulfur interacts with the pyridinic nitrogen, the sulfur atom loses electrons, while the nitrogen atom gains electrons; the charge transfer is along the carbon backbone, as shown in Fig. 4(a). The intramolecular charge transfer affects the resonance effect in conjugated polymers, which may help to stabilize the quinoid structure and reduce the band gaps [34]. For example, Figure 4(a) shows the aromatic and quinoid forms of the polymer NC_{S-N}-1 with the sulfur-nitrogen interaction. The single and double bonds of the thiophene ring in the aromatic structure become the double and single bonds in the quinoid structure, respectively, so the corresponding bond lengths may change if there is more quinoid character. Figure 4 (b) shows the correlation between the

6

bond length change (Δr) and the band gap change (ΔE_g), suggesting that the more quinoid character helps to reduce the band gap, which is consistent with Brédas' findings in polyaromatic molecules [34]. Thus, the sulfur-nitrogen interaction induces the intramolecular charge transfer in polymers, which increases the quinoid character and reduces the band gaps.

The sulfur-nitrogen pair has the largest charge transfer among all the noncovalent interactions studied here (see Table SII in the supporting information), so it affects band gaps and hole transfer rates more than other noncovalent atom pairs. When the thiophene sulfur interacts with the pyridinic nitrogen, the sulfur atom loses about 0.062±0.04 electrons and the nitrogen atom gains about 0.034±0.007 electrons. If we replace the sulfur atom in the thiophene moiety by the oxygen atom, i.e., thiophene becoming furan (see Fig. S4 in the supporting information), the oxygen atom loses about 0.039 ±0.007 electrons and the nitrogen atom may gain as little as 0.010 electrons or even lose 0.022 electrons. The oxygen atom is more electronegative than either the sulfur or the nitrogen atoms, so it is difficult for the oxygen atom to donate electrons to the C-C bonds, which explains why the oxygen-nitrogen pair does not have the similar intramolecular charge transfer as the sulfur-nitrogen pair. As a result, the quinoid character does not increase obviously with the oxygen-nitrogen interaction, and the band gaps and hole transfer rates do not change much.

For the sulfur-oxygen interaction, when the thiophene sulfur interacts with the benzodifuran oxygen, the transferred charge is very small, so it changes band gaps and hole transport rates little. When the fluorine atom interacts with the sulfur, nitrogen, or oxygen atoms as shown in Fig. 1, it loses electrons. Although the fluorine atom may increase the planarity of polymers and enhance the charge separation, it does not increase the quinoid character, so the noncovalent interactions with the fluorine atom change electronic properties little.

The effects of noncovalent interactions on the photovoltaic performance of polymers can be also found in experiment. Liu et al. reported that two planar polymers, P3TEA and P3TAE, differ only by the position of carboxyl side chains (see Fig. 5), but have different

electronic properties and OSC performance [35]. Our DFT calculations show that the band gap of P3TEA is smaller than that of P3TAE by 0.08 eV, which is consistent with the experimental optical gap change ($\sim$0.05 eV) [35]. Additionally, when a hole hops between two nearest 5,6-difluoro-2,1,3-benzothiadiazole (ffBT) moieties, the calculated transfer rate of P3TEA is larger than that of P3TAE by 10^6 times. When Liu et al. blended P3TEA with various molecular acceptors to make OSC devices, its narrower gap and faster charge transfer lead to the high photovoltaic performance [35–38]. Both P3TEA and P3TAE have the sulfur-nitrogen interaction, except that the carboxyl side chain in P3TAE is next to the sulfur-nitrogen pair. The Mulliken population analysis in Fig. 5(c) shows that the pyridinic nitrogen atom in P3TAE becomes less negatively charged than that in P3TEA by about 0.02 e due to the presence of the oxygen atom, so the quinoid character of P3TAE backbone increases less than that of P3TEA, which explains why P3TAE has a larger band gap and worse OSC performance.

CONCLUSION

Here, we applied the unconstrained and constrained DFT method to study six noncovalent intramolecular interactions typically found in the polymers in organic solar cell applications. Besides conformational control, we found that most of the noncolvalent interactions reduce the band gaps of polymers and increase the hole transfer rates, and the sulfur-nitrogen pair has the largest effect, which is not due to the enhancement of molecular planarity. The enhancement of electronic properties can be attributed to the intramolecular charge transfer, which increases the quinoid character of conjugated polymers. Our findings are also consistent with the experimental data. Our study suggests that choosing suitable noncovalent intramolecular interactions may further manipulate the electronic properties of planar polymers. This work paves the way for understanding the electronic structure of polymers, and suggests a new mechanism to design high-performance polymers for small-molecule-polymer

and all-polymer solar cells.

METHOD

We conducted first-principles calculations using the Quickstep module of the CP2K program package with a dual basis of Gaussian orbitals and plane waves [39]. We used the Goedecker-Teter-Hutter norm-conserving pseudopotentials for the valence electrons [40, 41]. A plane-wave density cutoff of 600 Ry was adopted. We used 3-dimensional periodic boundary conditions to simulate polymers, whose backbone chains are along the z direction. The vacuum along the x and y directions is at least 20 Å thick. We applied the molecularly optimized Gaussian basis sets of double zeta plus polarization quality (DZVP-MOLOPT) [42] and the Perdew-Burke-Ernzerhof (PBE) [43] exchange-correlation (xc) functional with Grimme's D3 dispersion correction [44] in the structural relaxation, where the force tolerance is 0.01 eV/Å. For the band gap and charge transfer calculations, we used Gaussian basis sets of triple zeta plus two sets of polarization functions (TZV2P) and the hybrid B3LYP xc functional [45–47].

DATA AVAILABILITY

The data that support this study are available upon request from the authors.

ACKNOWLEDGEMENTS

COMPETING INTERESTS

The authors declare no competing interests.

———————

* dingpan@ust.hk

[1] Serap Günes, Helmut Neugebauer, and Niyazi Serdar Sariciftci, "Conjugated polymer-based organic solar cells," Chem. Rev. **107**, 1324–1338 (2007).

[2] Luyao Lu, Tianyue Zheng, Qinghe Wu, Alexander M Schneider, Donglin Zhao, and Luping Yu, "Recent advances in bulk heterojunction polymer solar cells," Chem. Rev. **115**, 12666–12731 (2015).

[3] Chang Liu, Kai Wang, Xiong Gong, and Alan J Heeger, "Low bandgap semiconducting polymers for polymeric photovoltaics," Chem. Soc. Rev. **45**, 4825–4846 (2016).

[4] Guangye Zhang, Jingbo Zhao, Philip CY Chow, Kui Jiang, Jianquan Zhang, Zonglong Zhu, Jie Zhang, Fei Huang, and He Yan, "Nonfullerene acceptor molecules for bulk heterojunction organic solar cells," Chem. Rev. **118**, 3447–3507 (2018).

[5] Jianquan Zhang, Huei Shuan Tan, Xugang Guo, Antonio Facchetti, and He Yan, "Material insights and challenges for non-fullerene organic solar cells based on small molecular acceptors," Nat. Energy **3**, 720–731 (2018).

[6] Jun Yuan, Yunqiang Zhang, Liuyang Zhou, Guichuan Zhang, Hin-Lap Yip, Tsz-Ki Lau, Xinhui Lu, Can Zhu, Hongjian Peng, Paul A Johnson, *et al.*, "Single-junction organic solar cell with

over 15% efficiency using fused-ring acceptor with electron-deficient core," Joule **3**, 1140–1151 (2019).

[7] Sha Liu, Jun Yuan, Wanyuan Deng, Mei Luo, Yuan Xie, Quanbin Liang, Yingping Zou, Zhicai He, Hongbin Wu, and Yong Cao, "High-efficiency organic solar cells with low non-radiative recombination loss and low energetic disorder," Nat. Photonics. **14**, 300–305 (2020).

[8] Can Zhu, Jun Yuan, Fangfang Cai, Lei Meng, Huotian Zhang, Honggang Chen, Jing Li, Beibei Qiu, Hongjian Peng, Shanshan Chen, *et al.*, "Tuning the electron-deficient core of a non-fullerene acceptor to achieve over 17% efficiency in a single-junction organic solar cell," Energy Environ. Sci. **13**, 2459–2466 (2020).

[9] Shuixing Li, Chang-Zhi Li, Minmin Shi, and Hongzheng Chen, "New phase for organic solar cell research: Emergence of y-series electron acceptors and their perspectives," ACS Energy Lett. **5**, 1554–1567 (2020).

[10] Yong Cui, Huifeng Yao, Ling Hong, Tao Zhang, Yabing Tang, Baojun Lin, Kaihu Xian, Bowei Gao, Cunbin An, Pengqing Bi, *et al.*, "Organic photovoltaic cell with 17% efficiency and superior processability," Natl. Sci. Rev. **7**, 1239–1246 (2020).

[11] Qishi Liu, Yufan Jiang, Ke Jin, Jianqiang Qin, Jingui Xu, Wenting Li, Ji Xiong, Jinfeng Liu, Zuo Xiao, Kuan Sun, *et al.*, "18% efficiency organic solar cells," Sci. Bull. **65**, 272–275 (2020).

[12] Tao Jia, Jiabin Zhang, Kai Zhang, Haoran Tang, Sheng Dong, Ching-Hong Tan, Xiaohui Wang, and Fei Huang, "All-polymer solar cells with efficiency approaching 16% enabled using a dithieno [3', 2': 3, 4; 2", 3": 5, 6] benzo [1, 2-c][1, 2, 5] thiadiazole (fdtbt)-based polymer donor," J. Mater. Chem. A. **9**, 8975–8983 (2021).

[13] Ruijie Ma, Jianwei Yu, Tao Liu, Guangye Zhang, Yiqun Xiao, Zhenghui Luo, Gaoda Chai, Yuzhong Chen, Qunping Fan, Wenyan Su, Gang Li, Ergang Wang, Xinhui Lu, Feng Gao, Bo Tang, and He Yan Yan, "All-polymer solar cells with over 16% efficiency and enhanced stability enabled by compatible solvent and polymer additives," Aggregate , e58 (2021).

[14] Sarah Holliday, Yilin Li, and Christine K Luscombe, "Recent advances in high performance donor-acceptor polymers for organic photovoltaics," Prog. Polym. Sci. **70**, 34–51 (2017).

[15] Hae Jung Son, Wei Wang, Tao Xu, Yongye Liang, Yue Wu, Gang Li, and Luping Yu, "Synthesis of fluorinated polythienothiophene-co-benzodithiophenes and effect of fluorination on the photovoltaic properties," J. Am. Chem. Soc. **133**, 1885–1894 (2011).

[16] Andrew C Stuart, John R Tumbleston, Huaxing Zhou, Wentao Li, Shubin Liu, Harald Ade, and Wei You, "Fluorine substituents reduce charge recombination and drive structure and morphology development in polymer solar cells," J. Am. Chem. Soc. **135**, 1806–1815 (2013).

[17] Nicolas Leclerc, Patricia Chávez, Olzhas A Ibraikulov, Thomas Heiser, and Patrick Lévêque, "Impact of backbone fluorination on π-conjugated polymers in organic photovoltaic devices: a review," Polymers **8**, 11 (2016).

[18] Qianqian Zhang, Mary Allison Kelly, Nicole Bauer, and Wei You, "The curious case of fluorination of conjugated polymers for solar cells," Acc. Chem. Res. **50**, 2401–2409 (2017).

[19] Nicholas E Jackson, Brett M Savoie, Kevin L Kohlstedt, Monica Olvera de la Cruz, George C Schatz, Lin X Chen, and Mark A Ratner, "Controlling conformations of conjugated polymers and small molecules: The role of nonbonding interactions," J. Am. Chem. Soc. **135**, 10475–10483 (2013).

[20] Matthew B. Goldey, Daniel Reid, Juan de Pablo, and Giulia Galli, "Planarity and multiple components promote organic photovoltaic efficiency by improving electronic transport," Phys. Chem. Chem. Phys. **18**, 31388–31399 (2016).

[21] Hui Huang, Lei Yang, Antonio Facchetti, and Tobin J. Marks, "Organic and Polymeric Semiconductors Enhanced by Noncovalent Conformational Locks," Chem. Rev. **117**, 10291–10318 (2017).

[22] Benzheng Xia, Kun Lu, Liu Yuan, Jianqi Zhang, Lingyun Zhu, Xiangwei Zhu, Dan Deng, Huan Li, and Zhixiang Wei, "A conformational locking strategy in linked-acceptor type polymers for organic solar cells," Polym. Chem. **7**, 1323–1329 (2016).

[23] Simiao Yu, Yusheng Chen, Lei Yang, Pan Ye, Jianfei Wu, Jianwei Yu, Shiming Zhang, Yongqian Gao, and Hui Huang, "Significant enhancement of photovoltaic performance through introducing S...N conformational locks," J. Mater. Chem. A. **5**, 21674–21678 (2017).

[24] Sunsun Li, Wenchao Zhao, Jianqi Zhang, Xiaoyu Liu, Zhong Zheng, Chang He, Bowei Xu, Zhixiang Wei, and Jianhui Hou, "Influence of covalent and noncovalent backbone rigidification strategies on the aggregation structures of a wide-band-gap polymer for photovoltaic cells," Chem. Mater. **32**, 1993–2003 (2020).

[25] Asif Mahmood, Ailing Tang, Xiaochen Wang, and Erjun Zhou, "First-principles theoretical designing of planar non-fullerene small molecular acceptors for organic solar cells: manipulation of noncovalent interactions," Phys. Chem. Chem. Phys. **21**, 2128–2139 (2019).

[26] A Bondi, "van der waals volumes and radii," J. Phys. Chem. **68**, 441–451 (1964).

[27] Gregory C Welch, Ronald C Bakus, Simon J Teat, and Guillermo C Bazan, "Impact of regiochemistry and isoelectronic bridgehead substitution on the molecular shape and bulk organization of narrow bandgap chromophores," J. Am. Chem. Soc. **135**, 2298–2305 (2013).

[28] Alessandro Troisi, "Charge transport in high mobility molecular semiconductors: Classical models and new theories," Chem. Soc. Rev. **40**, 2347–2358 (2011).

[29] Benjamin Kaduk, Tim Kowalczyk, and Troy Van Voorhis, "Constrained density functional theory," Chem. Rev. **112**, 321–370 (2012).

[30] Nico Holmberg and Kari Laasonen, "Efficient constrained density functional theory implementation for simulation of condensed phase electron transfer reactions," J. Chem. Theory Comput. **13**, 587–601 (2017).

[31] Axel D Becke, "A multicenter numerical integration scheme for polyatomic molecules," J. Chem. Phys **88**, 2547–2553 (1988).

[32] Jean-Luc Brédas, David Beljonne, Veaceslav Coropceanu, and Jérôme Cornil, "Charge-transfer and energy-transfer processes in π-conjugated oligomers and polymers: a molecular picture," Chem. Rev. **104**, 4971–5004 (2004).

[33] David L Cheung and Alessandro Troisi, "Theoretical study of the organic photovoltaic electron acceptor pcbm: Morphology, electronic structure, and charge localization," J. Phys. Chem. C. **114**, 20479–20488 (2010).

[34] J. L. Brédas, "Relationship between band gap and bond length alternation in organic conjugated polymers," J. Chem. Phys. **82**, 3808–3811 (1985).

[35] Jing Liu, Lik-Kuen Ma, Fu Kit Sheong, Lin Zhang, Huawei Hu, Jing-Xuan Zhang, Jianquan Zhang, Zhengke Li, Chao Ma, Xu Han, *et al.*, "Carboxylate substitution position influencing polymer properties and enabling non-fullerene organic solar cells with high open circuit voltage and low voltage loss," J. Mater. Chem. A. **6**, 16874–16881 (2018).

[36] Jing Liu, Shangshang Chen, Deping Qian, Bhoj Gautam, Guofang Yang, Jingbo Zhao, Jonas Bergqvist, Fengling Zhang, Wei Ma, Harald Ade, *et al.*, "Fast charge separation in a nonfullerene organic solar cell with a small driving force," Nat. Energy **1**, 1–7 (2016).

[37] Jianquan Zhang, Yunke Li, Jiachen Huang, Huawei Hu, Guangye Zhang, Tingxuan Ma, Philip CY Chow, Harald Ade, Ding Pan, and He Yan, "Ring-fusion of perylene diimide acceptor enabling efficient nonfullerene organic solar cells with a small voltage loss," J. Am. Chem. Soc. **139**, 16092–16095 (2017).

[38] Jianquan Zhang, Fujin Bai, Yunke Li, Huawei Hu, Bin Liu, Xinhui Zou, Han Yu, Jiachen Huang, Ding Pan, Harald Ade, *et al.*, "Intramolecular π-stacked perylene-diimide acceptors for non-fullerene organic solar cells," J. Mater. Chem. A. **7**, 8136–8143 (2019).

[39] Joost VandeVondele, Matthias Krack, Fawzi Mohamed, Michele Parrinello, Thomas Chassaing, and Jürg Hutter, "Quickstep: Fast and accurate density functional calculations using a mixed Gaussian and plane waves approach," Comput. Phys. Commun. **167**, 103–128 (2005).

[40] M. Krack, "Pseudopotentials for H to Kr optimized for gradient-corrected exchange-correlation functionals," Theor. Chem. Acc. **114**, 145–152 (2005).

[41] Luigi Genovese, Thierry Deutsch, Alexey Neelov, Stefan Goedecker, and Gregory Beylkin, "Efficient solution of Poisson's equation with free boundary conditions," J. Chem. Phys. **125**,

074105 (2006).

[42] Joost VandeVondele and Jürg Hutter, "Gaussian basis sets for accurate calculations on molecular systems in gas and condensed phases," J. Chem. Phys. **127**, 114105 (2007).

[43] John P. Perdew, Kieron Burke, and Matthias Ernzerhof, "Generalized Gradient Approximation Made Simple," Phys. Rev. Lett. **77**, 3865–3868 (1996).

[44] Stefan Grimme, Jens Antony, Stephan Ehrlich, and Helge Krieg, "A consistent and accurate ab initio parametrization of density functional dispersion correction (DFT-D) for the 94 elements H-Pu," J. Chem. Phys. **132**, 154104 (2010).

[45] Axel D Becke, "A new mixing of hartree–fock and local density-functional theories," J. Chem. Phys. **98**, 1372–1377 (1993).

[46] P. J. Stephens, F. J. Devlin, C. F. Chabalowski, and M. J. Frisch, "Ab Initio Calculation of Vibrational Absorption and Circular Dichroism Spectra Using Density Functional Force Fields," J. Phys. Chem. **98**, 11623–11627 (1994).

[47] Chengteh Lee, Weitao Yang, and Robert G. Parr, "Development of the Colle-Salvetti correlation-energy formula into a functional of the electron density," Phys. Rev. B. **37**, 785–789 (1988).
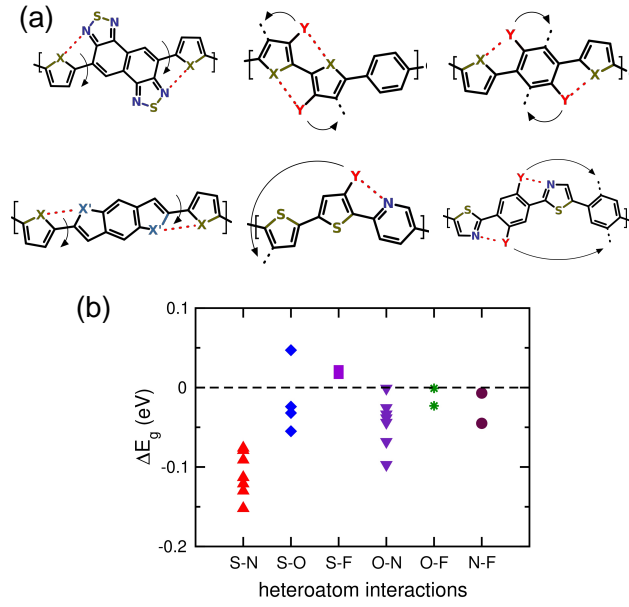
FIG. 1. Polymer structures and band gap change. (a) The planar polymer structures with the noncovalent interactions labelled by the dashed lines: S-N, S-O, S-F, O-N, O-F, and N-F. X or X' denotes the S or O atom, and Y is the F atom or the -OCH$_3$ group. The arrows show that we break up the noncovalent interactions by rotating moieties by 180° or swapping side chains, while still keeping the planar structures. (b) The change of band gaps after introducing the noncovalent interactions.
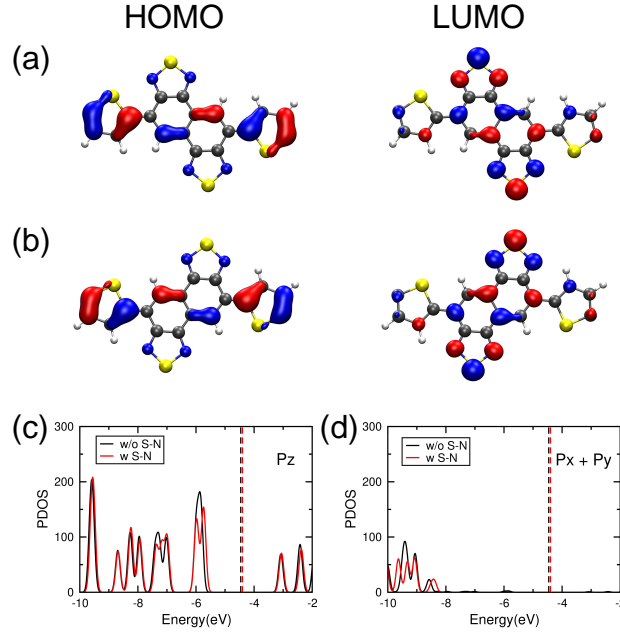
FIG. 2. Molecular orbitals and projected densities of states (PDOS) (a) HOMO and LUMO of the polymer NC_{S-N}-1 with the sulfur-nitrogen noncovalent interaction (w S-N). (b) HOMO and LUMO of the polymer HB-1 without the sulfur-nitrogen noncovalent interaction (w/o S-N). (c) PDOS on the p_z orbital of the conjugated carbon atoms in the polymers NC_{S-N}-1 and HB-1. (d) PDOS on the p_x and p_y orbitals of the conjugated carbon atoms in the polymers NC_{S-N}-1 and HB-1. The red and black dashed lines are the Fermi levels in the polymers NC_{S-N}-1 and HB-1, respectively. The energy levels are aligned using the vacuum energy level as the zero energy reference.
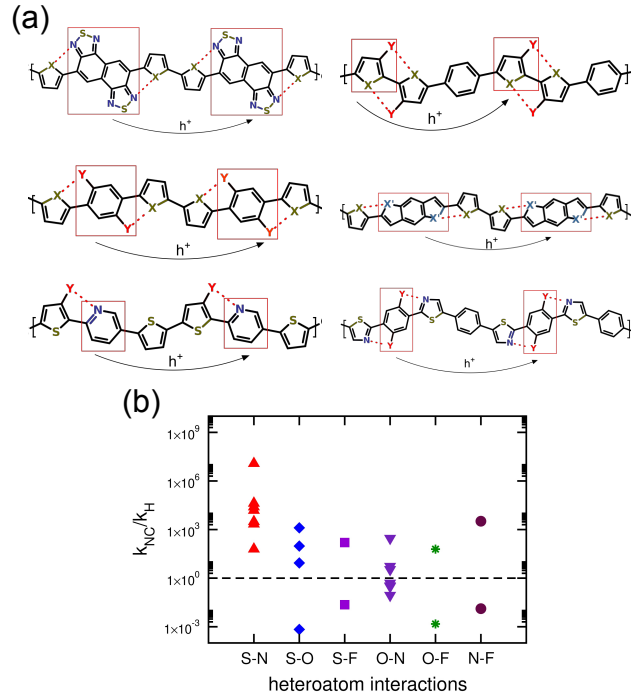
FIG. 3. Hole hopping pathways and transfer rates. (a) The pathways show that holes hop from the moieties involved in the noncovalent interactions to the same moieties in the adjoining repeat units in the polymers. (b) The ratio of hole transfer rates (k_{NC}/k_H) between the polymers with and without the noncovalent interactions.
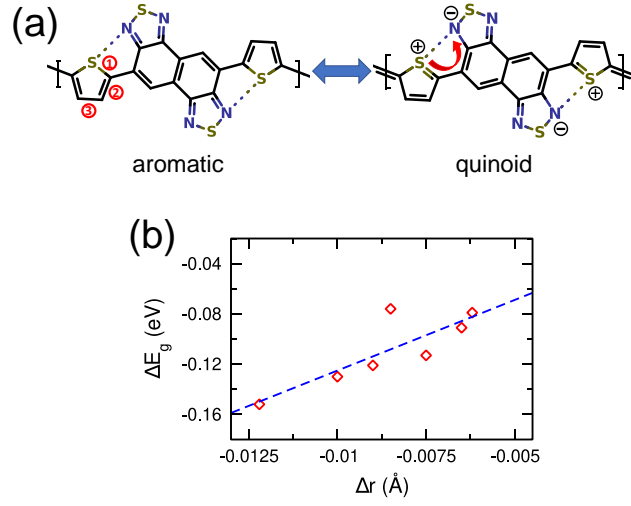
FIG. 4. Resonance structures and the decrease of polymer band gaps. (a) Aromatic and quinoid structures of the polymer NC_{S-N}-1 with the sulfur-nitrogen interaction. (b) After the noncovalent interactions form, the change of polymer band gaps, ΔE_g, as a function of Δr. r is calculated as $r = d_① - d_② + d_③$, where $d_①$, $d_②$, and $d_③$ are the S-C, C=C, and C-C bond lengths in the thiophene moiety. The dashed line shows the linear fit.
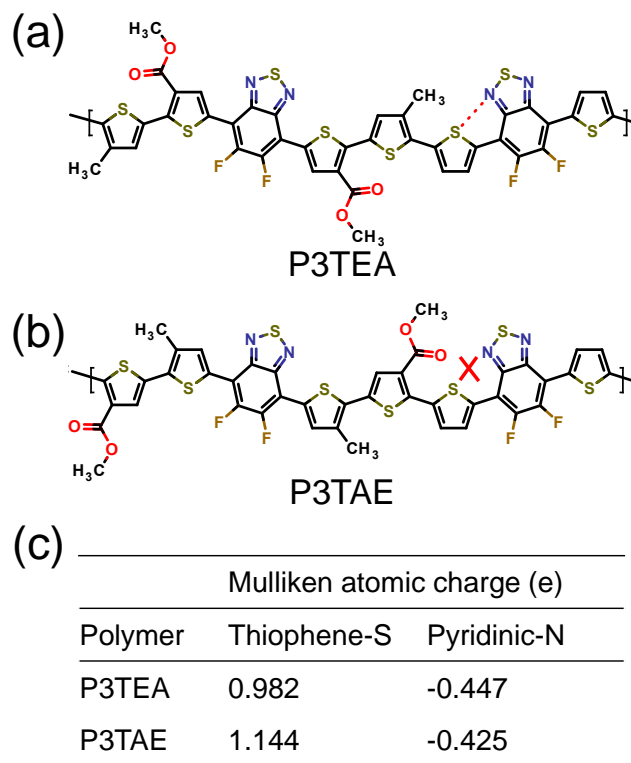
FIG. 5. Structures of the polymers (a) P3TEA and (b) P3TAE. (c) Mulliken atomic charges of the thiophene sulfur atom and the pyridinic nitrogen atom in P3TEA and P3TAE.

Supporting information

Bin Liu,[1] Dario Rocca,[2] He Yan,[3] and Ding Pan[1,3,4,*]

[1]*Department of Physics, Hong Kong University*

of Science and Technology, Hong Kong, China

[2]*Université de Lorraine & CNRS, Laboratoire de Physique*

et Chimie Théoriques (LPCT), F-54000 Nancy, France

[3]*Department of Chemistry, The Hong Kong University*

of Science and Technology, Hong Kong, China

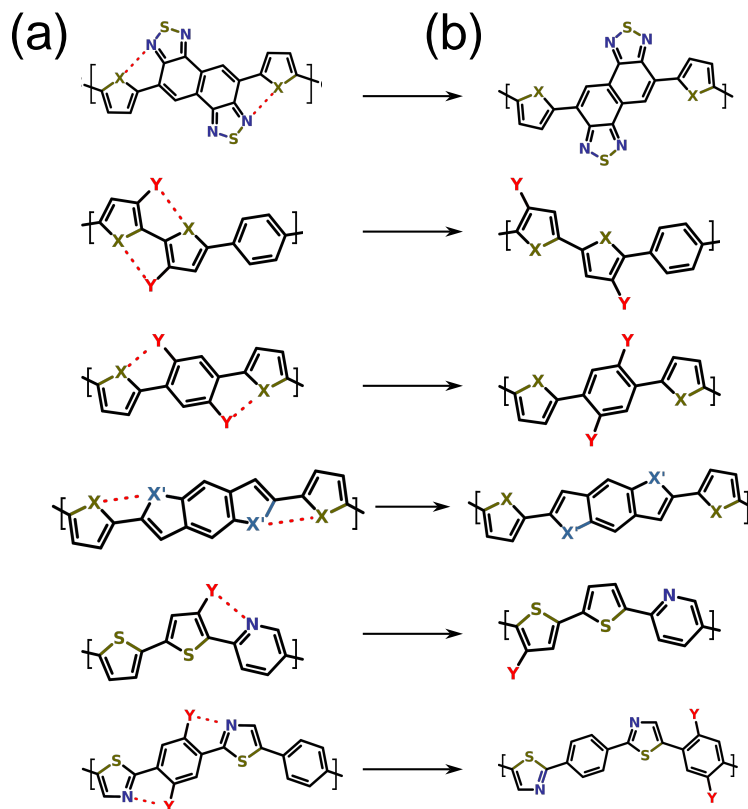[4]*HKUST Fok Ying Tung Research Institute, Guangzhou, China*

FIG. S1. Polymer structures (a) with the noncovalent interactions (dashed lines) and (b) without the noncovalent interactions. X or X' are the S or O atom, and Y is the F atom or the -OCH$_3$ group. We break up the noncovalent interactions by rotating moieties by 180° or swapping side chains. All the polymers have the planar structure.
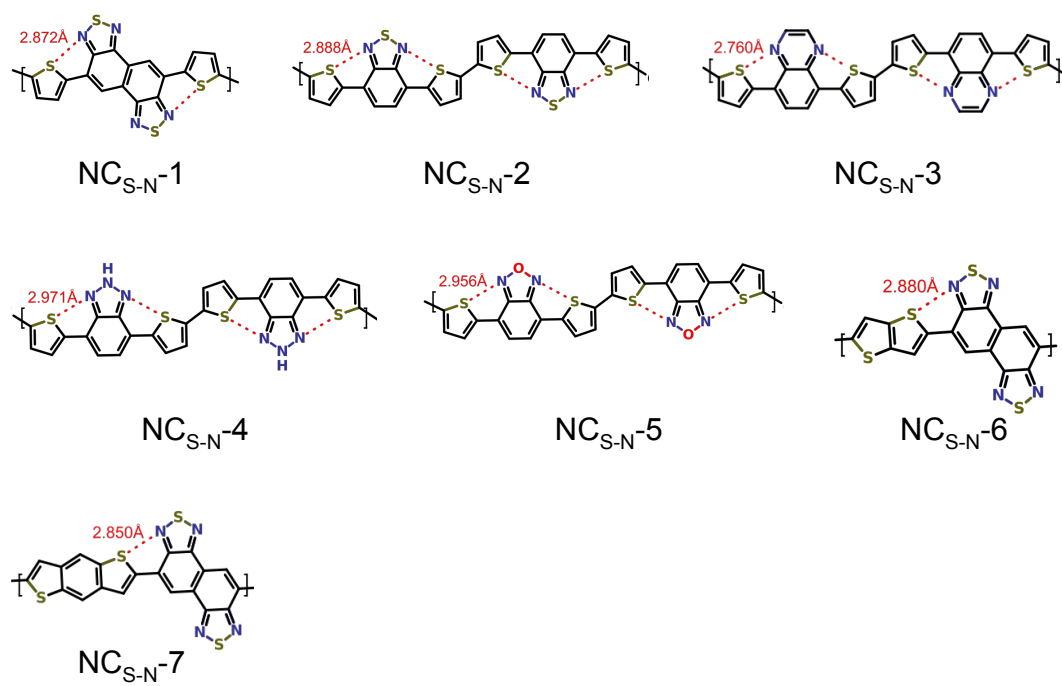
FIG. S2. Seven polymer structures with the sulfur-nitrogen interaction.

---

* dingpan@ust.hk

HB-1   HB-2   HB-3
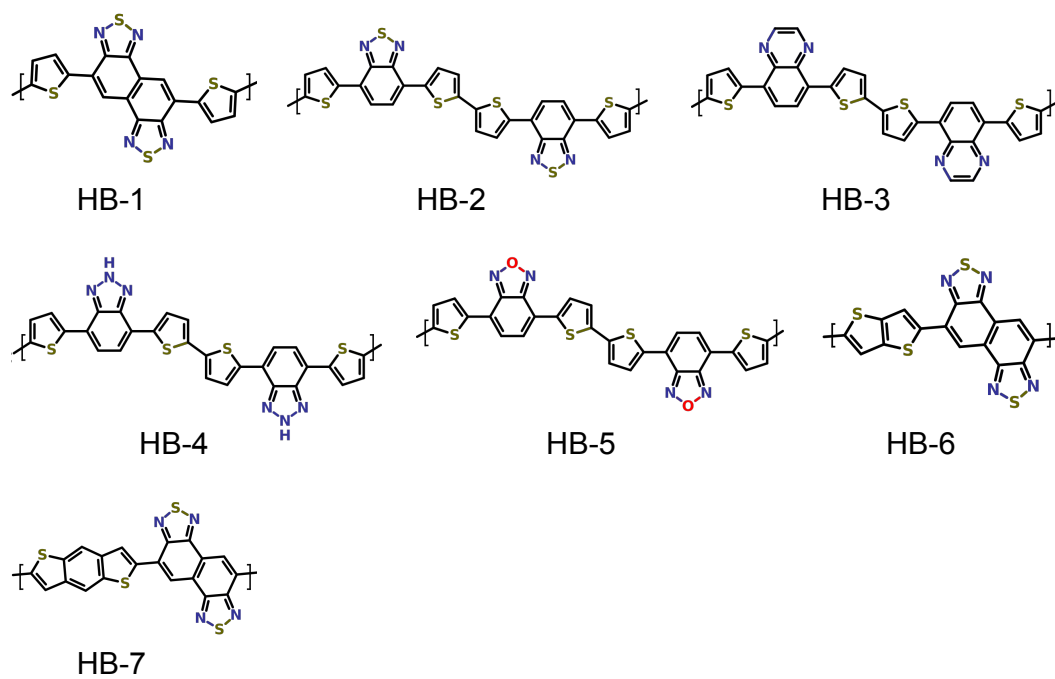
HB-4   HB-5   HB-6

HB-7

FIG. S3. Seven polymer structures without the sulfur-nitrogen interaction obtained by rotating the moieties or swapping the side chains in the structures in Fig. S2.
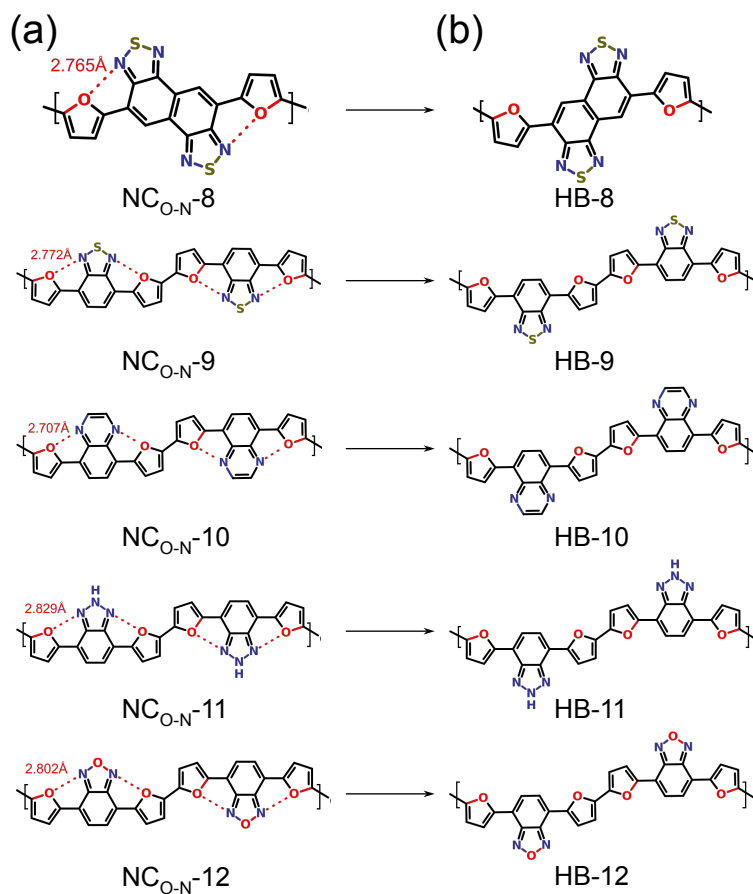
FIG. S4. Polymer structures (a) with and (b) without the oxygen-nitrogen interaction.
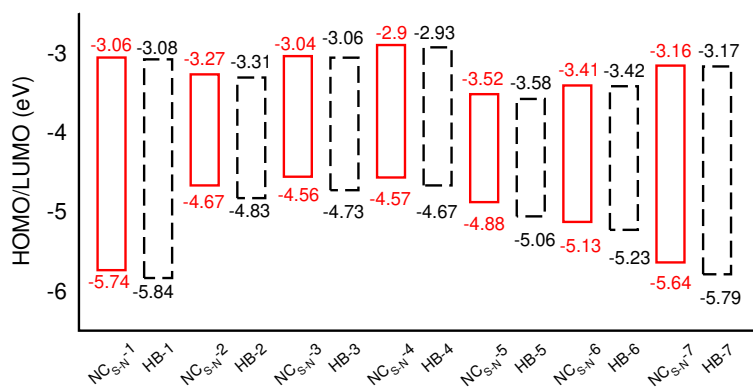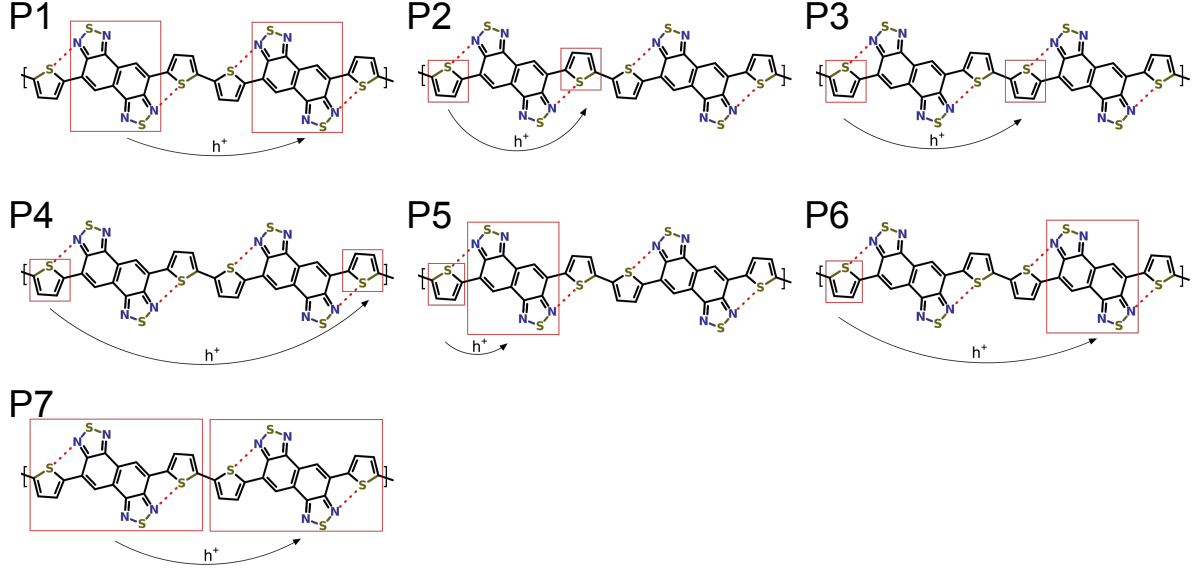

FIG. S5. HOMO and LUMO levels of the polymers with and without the sulfur-nitrogen interaction. The polymer structures are shown in Fig. S2 and S3. The energy levels are aligned using the vacuum energy level as the zero energy reference.

FIG. S6. Non-adiabatic electronic couplings , H_{AB}, of seven hopping pathways in the polymers with ((NC$_{S-N}$-1 ~ NC$_{S-N}$-5)) and without (HB-1 ~ HB-5) the sulfur-nitrogen interaction. The unit is eV.

Polymer	Hopping Pathway						
	P1	P2	P3	P4	P5	P6	P7
NC$_{S-N}$-1	2.12	2.20	2.05	4.38	3.32	2.36	1.98
HB-1	1.83	2.07	1.95	4.35	3.25	2.16	1.78
NC$_{S-N}$-2	2.56	2.44	2.19	4.14	3.81	2.61	1.85
HB-2	2.30	2.31	2.08	4.12	3.82	2.45	1.73
NC$_{S-N}$-3	2.84	2.32	2.09	4.13	3.80	2.67	1.80
HB-3	2.41	2.20	2.00	4.11	3.87	2.49	1.65
NC$_{S-N}$-4	2.37	2.46	2.22	4.21	4.01	2.63	1.85
HB-4	2.17	2.34	2.11	4.17	3.94	2.44	1.75
NC$_{S-N}$-5	2.68	2.41	2.16	4.09	3.87	2.65	1.81
HB-5	2.44	2.31	2.07	4.08	3.88	2.49	1.74
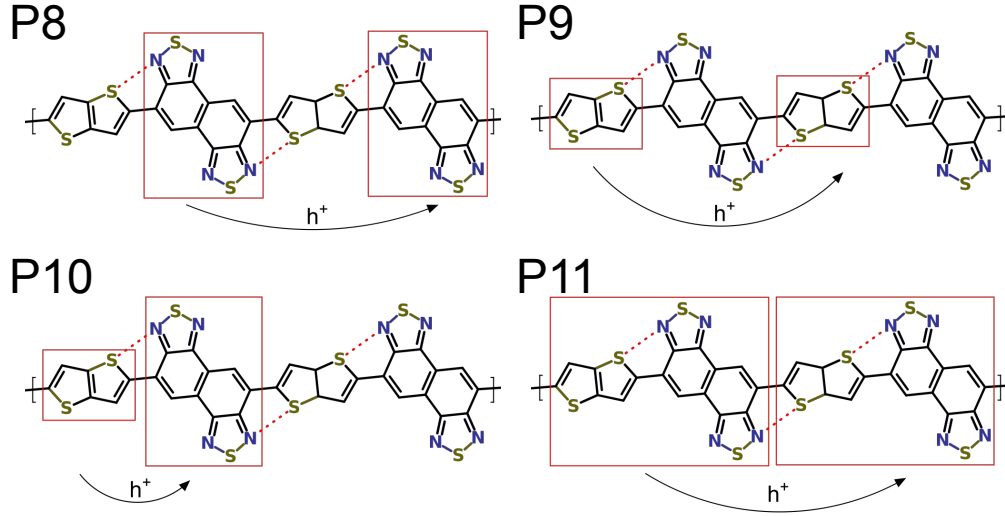
Polymer	Hopping Pathway			
	P8	P9	P10	P11
NC_{S-N}-6	1.88	1.32	2.44	1.57
HB-6	1.75	1.28	2.32	1.52
NC_{S-N}-7	1.76	0.87	1.66	1.21
HB-7	1.55	0.81	1.58	1.19

FIG. S7. Non-adiabatic electronic couplings , H_{AB}, of four hopping pathways in the polymers with $((NC_{S-N}$-6 and NC_{S-N}-7)) and without (HB-6 and HB-7) the sulfur-nitrogen interaction. The unit is eV.

TABLE SI. Reorganization energies, λ, and hole hopping rates, k^{Troisi}, obtained by the Troisi rate equation. We compared the pathway P1 for the polymers NC_{S-N}-1 ~ NC_{S-N}-5 and HB-1 ~ HB-5, and the pathway P8 for the polymers NC_{S-N}-6, NC_{S-N}-7, HB-6, and HB-7.

Polymer	$\lambda(eV)$	$k^{Troisi}(s^{-1})$
NC_{S-N}-1	0.47	2.16×10^{47}
HB-1	0.4	5.09×10^{42}
NC_{S-N}-2	0.52	3.75×10^{54}
HB-2	0.49	2.43×10^{50}
NC_{S-N}-3	0.63	6.51×10^{58}
HB-3	0.59	5.41×10^{51}
NC_{S-N}-4	0.54	1.78×10^{51}
HB-4	0.56	5.735×10^{47}
NC_{S-N}-5	0.52	4.44×10^{56}
HB-5	0.57	1.76×10^{52}
NC_{S-N}-6	0.64	3.02×10^{42}
HB-6	0.57	4.8×10^{40}
NC_{S-N}-7	0.36	5.93×10^{41}
HB-7	0.29	2.71×10^{38}

TABLE SII. Change of Mulliken atomic charges after introducing the noncovalent interactions between the atoms X and Y. The positive values mean that the atoms are losing electrons and thus more positively charged.

X-Y	Change of Mulliken atomic charge (e)	
	X	Y
S-N	0.0616±0.0400	-0.0335±0.0070
S-O	0.0097±0.0744	-0.0089±0.0066
S-F	0.0330±0.0130	0.0040±0.0010
O-N	0.0394±0.0067	0.0062±0.0158
O-F	0.0166±0.0030	0.0159±0.0002
N-F	0.0420±0.0060	0.0364±0.0023